

The Predicament of Absorption-dominated Reionization II: Observational Estimate of the Clumping Factor at the End of Reionization

FREDERICK B. DAVIES,¹ SARAH E. I. BOSMAN,^{2,1} AND STEVEN R. FURLANETTO³

¹*Max-Planck-Institut für Astronomie, Königstuhl 17, D-69117 Heidelberg, Germany*

²*Institute for Theoretical Physics, Heidelberg University, Philosophenweg 12, D-69120, Heidelberg, Germany*

³*Department of Physics & Astronomy, University of California, Los Angeles, CA 90095, USA*

ABSTRACT

The history of reionization reflects the cumulative injection of ionizing photons by sources and the absorption of ionizing photons by sinks. The latter process is traditionally described in terms of a “clumping factor” which encodes the average quadratic increase in the recombination rate of dense gas within the cosmic web. The recent measurement of a short mean free path of ionizing photons from stacked quasar spectra at $z \simeq 6$ has placed the importance of sinks under increased scrutiny, but its connection to the recombination rate is not immediately obvious. Here we present analytic arguments to connect the clumping factor to the mean free path by invoking ionization equilibrium within the ionized phase of the intergalactic medium at the end of (and after) reionization. We find that the latest mean free path and hydrogen photoionization rate measurements at $z = 5\text{--}6$ imply a global clumping factor $C \approx 12$, much higher than previous determinations from radiation-hydrodynamic simulations of the reionization process. Similar values of C are also derived when applying the same procedure to observations at $2 < z < 5$. Compared to the traditional assumption of $C = 3$, high-redshift galaxies must produce roughly twice as many ionizing photons (≈ 3 photons per baryon) to reionize the universe by $z \sim 6$. This additional requirement on the ionizing photon budget may help to reconcile the reionization history with JWST observations that suggest a far greater output of ionizing photons by the most distant galaxy populations.

Keywords: Intergalactic medium(813), Reionization(1383)

1. INTRODUCTION

After the formation of baryons during the Big Bang, and their subsequent (re-)combination into atoms and the release of the cosmic microwave background (CMB), the hydrogen and helium in the Universe persisted in a predominantly neutral state. After the formation of the first stars and galaxies, the ionizing photons emitted by massive stars began to carve ionized bubbles into the surrounding intergalactic medium (IGM), beginning the epoch of reionization. The ionized bubbles from individual galaxies eventually merged (Furlanetto et al. 2004), filling more and more of the cosmic volume until, by $z \sim 5.3$ (Bosman et al. 2022), the IGM was fully reionized.

The most straightforward quantitative description of reionization was put forward by Madau et al. (1999), whose “one-zone” model for the process provides valuable intuition:

$$\frac{dQ}{dt} = \frac{\dot{n}_{\text{ion}}}{\langle n_{\text{H}} \rangle} - \frac{Q}{t_{\text{rec}}}, \quad (1)$$

where Q is the ionized fraction of the IGM, and the first and second terms on the right-hand side represent the source and sink terms, respectively. The sources are represented by \dot{n}_{ion} , the emissivity of ionizing photons, while the sinks are represented by t_{rec} , the recombination timescale of the ionized gas. In this work, as in Madau et al. (1999), we will assume that Q represents the *volume-averaged* ionized fraction. While the inside-out nature of reionization implies that a mass-averaged approach may be more appropriate, in which case an additional factor of Q arises in the sink term (e.g. Chen et al. 2020), equation (1) is approximately correct in a two-phase approximation (cf. Wu et al. 2021) where the IGM is either fully ionized ($x_{\text{HII}} = 1$) or neutral ($x_{\text{HII}} = 0$). That is, Q represents the volume of the IGM *within the ionized phase* rather than a physical ionized fraction, and so it does not asymptote to a finite residual neutral fraction after reionization is complete (although see Madau 2017 for a solution to this).

Considerable effort has been undertaken to determine \dot{n}_{ion} at early cosmic time. Such determinations typically involve a measurement of the UV luminosity function (LF) of galaxies at high redshifts ($z > 6$), but the connection between the UV LF and the ionizing output of galaxies is still uncertain. This connection is usually parameterized as

$$\dot{n}_{\text{ion}} = \rho_{\text{UV}} \xi_{\text{ion}} f_{\text{esc}}, \quad (2)$$

where ρ_{UV} is the integral over the UV LF down to some magnitude limit, ξ_{ion} is the ‘‘ionizing efficiency’’ which represents the average (intrinsic) spectral shape of the stellar populations between the ionizing and non-ionizing UV continuum, and f_{esc} is the escape fraction of ionizing photons from the galaxies into the IGM. While observations of galaxy nebular emission lines can constrain their ξ_{ion} (e.g. Ning et al. 2023; Prieto-Lyon et al. 2023; Simmonds et al. 2023, 2024; Atek et al. 2024), direct measurements of f_{esc} (i.e., direct detections of ionizing photons) are hindered by the high opacity of the Lyman-series forests, and thus are only possible at redshifts $z \lesssim 4$ (e.g. Izotov et al. 2016; Vanzella et al. 2018; Ji et al. 2020; Pahl et al. 2021).

The role of sinks has been a subject of considerable debate over the years. As mentioned above, sinks of ionizing photons enter the Madau et al. (1999) formalism via t_{rec} , the average recombination time of a proton in the IGM, which can be written as

$$t_{\text{rec}} = \frac{1}{C \langle n_{\text{H}} \rangle \alpha_{\text{HII}}(T)}, \quad (3)$$

where α_{HII} is the hydrogen recombination rate, and $\langle n_{\text{H}} \rangle$ is the mean cosmic hydrogen density. Crucially, as recombination is a collisional process, the rate depends on the squared density of ionized gas. It is common to summarize this dependence with the so-called ‘‘clumping factor,’’

$$C \equiv \langle n^2 \rangle / \langle n \rangle^2, \quad (4)$$

such that $t_{\text{rec}} = t_{\text{rec}}^{\text{uniform}} / C$. As there is no analytic shortcut to fully determine C from first principles, the assumed value is typically derived from cosmological simulations.

Early cosmological hydrodynamical simulations suggested $C \sim 30$ (e.g. Gnedin & Ostriker 1997), implying a dominant role of recombinations in determining the reionization history. However, this high value considered all gas particles in the simulation volume. In practice, recombinations occurring *inside* of galaxies are already accounted for by the f_{esc} parameter, so care must be taken to avoid double-counting. Later works by Iliev et al. (2005, 2007) and Raićević & Theuns (2011) took

this exclusion into account and found values closer to $C \sim 10$, albeit using dark-matter-only N-body simulations. But the baryons are also subject to gas pressure, which smooths their distribution relative to the dark matter field. Following several works employing radiation hydrodynamic simulations of reionization (Pawlik et al. 2009; Shull et al. 2012; Finlator et al. 2012, see also McQuinn et al. 2011), a value of $C \sim 2\text{--}3$ is now a typical assumption in analytic reionization models in the literature. That said, more recent simulations suggest a value of C higher by a factor of ~ 2 (e.g. Chen et al. 2020; Kannan et al. 2022).

The impact of sinks is now being revisited after the measurement of a short mean free path of ionizing photons at $z = 6$ by Becker et al. (2021), and further confirmed by Zhu et al. (2023, see also Bosman 2021; Satyavolu et al. 2023), which suggests the presence of substantially more small-scale structure in the IGM than present in traditional reionization simulations. A short mean free path can dramatically increase the number of ionizing photons required to ionize the IGM, as photons must travel long distances from ionizing sources to large-scale voids (Davies et al. 2021, henceforth Paper I, see also Cain et al. 2021). However, the quantitative connection between the short mean free path and the clumping factor is not immediately obvious (e.g. Cain et al. 2023), which has limited the extent to which the short mean free path has been taken into account by the larger reionization community.

In this work, we aim to build a stronger connection between the mean free path and clumping factor at high redshift, in an attempt to unify the description of ionizing photon sinks during the reionization epoch. We first show that the clumping factor at a given redshift can be estimated from the ionizing background intensity and mean free path. We then apply this methodology to measurements of these quantities across cosmic time, finding a nearly constant value of C which is several times higher than typically assumed.

We assume a *Planck* Λ CDM cosmology (Planck Collaboration et al. 2020) with $h = 0.68$, $\Omega_m = 0.31$, and $\Omega_b = 0.049$.

2. THE CLUMPING FACTOR AND THE MEAN FREE PATH

In this section, we will investigate the connection between the clumping factor and the mean free path of ionizing photons. But first, we must define what we mean by ‘‘clumping factor,’’ as its exact definition varies considerably between different works. Here we define the clumping factor to be the relevant clumping factor for solving equation (1) – i.e. the clumping factor

that provides the correct globally averaged recombination rate, but where effects inside of galaxies that give rise to the escape fraction in the definition of \dot{n}_{ion} are ignored. Specifically, we assume that C is the constant of proportionality between the true global (external) recombination rate $\dot{n}_{\text{rec}} = \langle n_e n_{\text{HII}} \alpha_{\text{HII}} \rangle$ and the recombination rate at the cosmic mean density,

$$C \equiv \frac{\langle n_e n_{\text{HII}} \alpha_{\text{HII}} \rangle}{\langle n_e \rangle \langle n_{\text{HII}} \rangle \langle \alpha_{\text{HII}} \rangle} \quad (5)$$

where we assume that the fiducial recombination coefficient in the denominator is equal to the Case B recombination rate for 10,000 K gas¹, $\langle \alpha_{\text{HII}} \rangle = \alpha_{\text{HII}}^B(T = 10,000 \text{ K})$.

The most straightforward way to connect the clumping factor to the mean free path starts with the assumption of photoionization equilibrium, which should generally hold in the ionized IGM,

$$n_{\text{HI}} \Gamma_{\text{HI}} = \langle n_e n_{\text{HII}} \alpha_{\text{HII}} \rangle = C \chi_e (1 - x_{\text{HI}})^2 n_{\text{H}}^2 \alpha_{\text{HII}}, \quad (6)$$

where Γ_{HI} is the photoionization rate of hydrogen and $\chi_e \approx 1.08$ is the enhancement in the number of free electrons due to ionized helium². Solving for C , we have

$$C = \frac{x_{\text{HI}} n_{\text{H}} \Gamma_{\text{HI}}}{\chi_e (1 - x_{\text{HI}})^2 n_{\text{H}}^2 \alpha_{\text{HII}}}. \quad (7)$$

The two unknowns in this expression are Γ_{HI} and x_{HI} . While the former can be derived from observations of the Ly α forest, and is most sensitive to low-density gas which is unambiguously resolved in simulations, the residual neutral fraction is not so simple to derive, as it is sensitive to self-shielding and geometrical effects in dense gas (e.g. [McQuinn et al. 2011](#); [Erkal 2015](#)).

To proceed, one can make the simplifying assumption that the neutral fraction is connected to the mean free path of ionizing photons via $\lambda_{\text{mfp}} = (n_{\text{HI}} \sigma_{\text{HI}})^{-1}$. In this case, similar to the “effective” clumping factor in [Cain et al. \(2023\)](#), we have:

$$C = \frac{\sigma_{\text{HI}} \Gamma_{\text{HI}}}{\lambda_{\text{mfp}} \chi_e (1 - x_{\text{HI}})^2 n_{\text{H}}^2 \alpha_{\text{HII}}}, \quad (8)$$

where we note that both the mean free path and photoionization cross section terms implicitly represent frequency-averaged values. This expression for the

¹ We note that $\alpha_{\text{HII}}^B(T = 10,000 \text{ K}) \simeq \alpha_{\text{HII}}^A(T = 20,000 \text{ K})$, another common assumption in previous works.

² We assume that helium is singly-ionized at the same time as hydrogen, and that the (second) reionization of helium has not yet begun. While this assumption will become incorrect at $z \lesssim 4$ (e.g. [Worseck et al. 2019](#)), the additional 8% boost to the electron density from the second ionization of helium is small compared to the uncertainties in the observed quantities we employ in § 3.2.

mean free path, however, makes the crucial assumption that neutral hydrogen is uniformly distributed in space. In reality, the dense self-shielded gas that gives rise to optically-thick absorption should be inhomogeneous, distributed in clumps and/or in the filaments of the cosmic web (e.g. [McQuinn et al. 2011](#)).

Another way to associate the clumping factor with the mean free path was suggested by [Emberson et al. \(2013\)](#), who connected the attenuation of ionizing photon flux to the recombination rate. In this model, one considers the attenuation of ionizing photon flux dF inside a slab of material with area dA and proper width ds compared to the recombinations inside said slab,

$$-dF dA = C n_e n_{\text{HII}} \alpha_{\text{HII}} dA ds, \quad (9)$$

where the flux inside the slab is attenuated following

$$\frac{dF}{ds} = -F(1+z)/\lambda_{\text{mfp}}, \quad (10)$$

where the $(1+z)$ term converts λ_{mfp} from comoving to proper units. The following expression can then be derived after solving for C ,

$$C = \frac{F(1+z)}{\lambda_{\text{mfp}} \chi_e (1 - x_{\text{HI}})^2 n_{\text{H}}^2 \alpha_{\text{HII}}}, \quad (11)$$

where we note again that the F and λ_{mfp} terms represent values integrated over the spectrum of the ionizing background. While this expression improves upon the previous one by removing the explicit connection between the mean free path and the neutral fraction, the geometrical assumption in its derivation (i.e. the slab) introduces additional ambiguity.

We suggest a third way to conceptualize (and quantify) the connection between the mean free path and the clumping factor. A typical ionizing photon passing through the IGM will travel one mean free path before being absorbed, i.e. before ionizing a hydrogen atom. Thus a “photon photo-ionization rate,” the rate at which a given ionizing photon will ionize a hydrogen atom, can be written as $\Gamma_\gamma = c/\lambda_{\text{mfp}}$. The space density of photoionizations is then $n_\gamma \Gamma_\gamma = n_\gamma \times c/\lambda_{\text{mfp}}$, where n_γ is the number density of ionizing photons. In ionization equilibrium, this rate will balance the recombination rate, i.e.

$$\frac{n_\gamma c}{\lambda_{\text{mfp}}} = C \alpha_{\text{HII}} \chi_e (1 - x_{\text{HI}})^2 n_{\text{H}}^2, \quad (12)$$

Solving for C as above, we find

$$C = \frac{n_\gamma c}{\lambda_{\text{mfp}} \alpha_{\text{HII}} \chi_e (1 - x_{\text{HI}})^2 n_{\text{H}}^2}, \quad (13)$$

where again the n_γ and λ_{mfp} terms represent frequency-averaged quantities.

In all three cases, the inferred clumping factor is proportional to the strength of the ionizing background (in various forms) divided by the mean free path of ionizing photons, e.g. $C \propto \Gamma_{\text{HI}}/\lambda_{\text{mfp}}$. All three methods result in quantitatively similar values for C ; in this work, we adopt the third method to compute C (i.e. equation 13), as it appears to have the fewest explicit assumptions on the nature of the distribution of neutral gas.

We have so far ignored the dependence on photon frequency of various quantities in the expressions for C above for the sake of clarity, but due to the steep frequency dependence of the photoionization cross-section (Verner et al. 1996), such terms could matter at the level of a factor of a few. We write the specific number density of ionizing photons n_ν as

$$n_\nu = \frac{u_\nu}{h\nu} = \frac{4\pi J_\nu}{c h\nu}, \quad (14)$$

where u_ν is the specific energy density and J_ν is the specific angle-averaged mean intensity of the ionizing background. We then proceed to estimate C using the following expression:

$$C = \left[4\pi \int_{\nu_{\text{HI}}}^{4\nu_{\text{HI}}} \frac{J_\nu}{h\nu\lambda_\nu} d\nu \right] \times \frac{1}{\alpha_{\text{HII}}\chi_e(1-x_{\text{HI}})^2 n_{\text{H}}^2}, \quad (15)$$

where ν_{HI} is the frequency of the hydrogen ionizing edge. In the following, we make the assumption that the neutral fraction is small enough that the $(1-x_{\text{HI}})$ term can be approximated as unity – that is, we compute the clumping factor relative to a fully ionized IGM. We further approximate the frequency dependencies of the mean free path and ionizing background intensity as power laws with $\lambda_\nu \propto \nu^{\alpha_\lambda}$ and $J_\nu \propto \nu^{-\alpha_b}$, leading to an analytic simplification to equation (15) as long as $\alpha_b + \alpha_\lambda \neq 0$,

$$C = \frac{4\pi J_{\text{HI}}}{h\nu_{\text{HI}}\lambda_{\text{mfp}}} \left[\frac{1 - 4^{-(\alpha_b + \alpha_\lambda)}}{\alpha_b + \alpha_\lambda} \right] \times \frac{1}{\alpha_{\text{HII}}\chi_e n_{\text{H}}^2}, \quad (16)$$

where J_{HI} and λ_{mfp} are $J_\nu(\nu_{\text{HI}})$ and $\lambda_\nu(\nu_{\text{HI}})$, respectively.

The frequency dependence assumptions are largely encapsulated by the term in brackets, which is a function of $\alpha_b + \alpha_\lambda$, equal to 2 with our assumed power-law indices³. In practice, as described below in § 3.2, we will

³ We note that at $z \gtrsim 5$, where the mean free path is short relative to the Hubble distance (the “absorption-limited” regime), we can write $J_\nu \propto \epsilon_\nu \lambda_\nu$ where ϵ_ν is the average ionizing emissivity (Meiksin & White 2003). The implied scaling of the emissivity is $\epsilon_\nu \propto \nu^{-(\alpha_b + \alpha_\lambda)}$, suggesting that our choice of $\alpha_b + \alpha_\lambda = 2$ is reasonable (e.g. Becker & Bolton 2013). Even harder ionizing spectra are also plausible for young, metal-poor stellar populations (e.g. D’Aloisio et al. 2019) which would increase our C estimates.

convert observational constraints on Γ_{HI} to J_{HI} , which introduces an additional factor dependent on α_b alone. Lower (higher) values of C would be derived if the ionizing background is softer (harder), or if the mean free path is a stronger (weaker) function of frequency. We discuss the behavior of the frequency dependence term further in Appendix A, and note that even in the most extreme case (corresponding to $\alpha_\lambda \approx 3$) our assumptions could only overestimate C by a factor of two.

As measurements of the ionizing background require non-zero transmission through the highly sensitive Ly α forest (Gunn & Peterson 1965), application of this method will only become possible at the very end of the reionization process. Thus the clumping factor during the majority of reionization cannot be constrained directly. At these earlier times, the inside-out nature of reionization should lead to higher densities in the ionized regions, and thus a higher recombination rate relative to the mean IGM (e.g. Chen et al. 2020, see also So et al. 2014). We ignore this effect for simplicity in our analytic calculations, but note that this would likely increase the effective clumping factor significantly at low ionized fractions as in Chen et al. (2020).

3. ESTIMATING THE CLUMPING FACTOR FROM IGM OBSERVATIONS

In this section, we use observational properties of the IGM to constrain the clumping factor as defined in the previous section. Here we stress that our clumping factor is an effective quantity corresponding to the entire volume of the IGM, and not a “local” clumping factor that can be applied to the density field in simulations a posteriori (see, e.g., Raičević & Theuns 2011; Kurov & Gnedin 2015). In particular, our definition of the clumping factor is specifically designed for use in analytic reionization calculations like equation (1) that consider the IGM as a whole (Madau et al. 1999).

3.1. Observations of Γ_{HI} and λ_{mfp}

Estimating the clumping factor using the method above requires an estimate of the ionizing background intensity as well as the mean free path of ionizing photons. While most studies of the clumping factor have focused on its behavior during the reionization epoch, our formalism applies to any cosmic time where both of these quantities have been measured.

For the mean free path, at $z < 5$ we use the power-law fit to the direct measurements of quasar spectra stacked beyond the Lyman limit from Worseck et al. (2014) and references therein. At $z > 5$, we use the measurements from Zhu et al. (2023), who (following Becker et al. 2021) use a similar stacking method to Worseck et al. (2014)

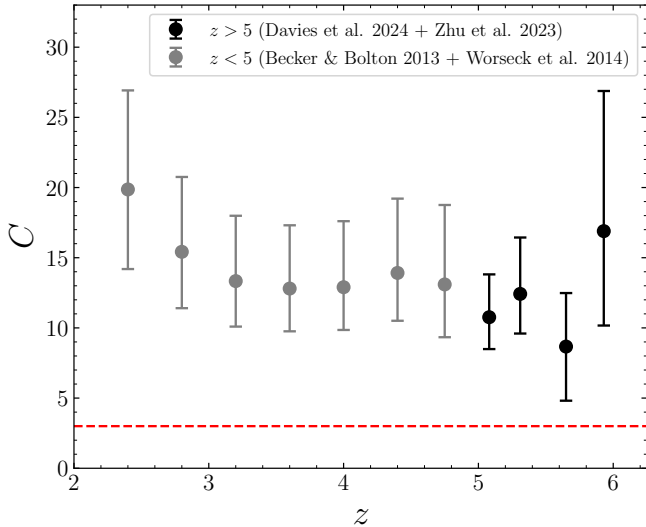


Figure 1. Clumping factor estimates applying equation (16) to constraints on the hydrogen photoionization rate Γ_{HI} (via equation 17) and ionizing photon mean free path λ_{mfp} . The grey points at $z < 5$ use Γ_{HI} from Becker & Bolton (2013) and λ_{mfp} from Worseck et al. (2014), while the black points at $z > 5$ use the corresponding constraints from Davies et al. (2024) and Zhu et al. (2023), respectively.

but additionally account for the bias due to the intense local ionizing flux from the background quasars. At all redshifts we assume a power-law frequency dependence of the mean free path of $\lambda_{\nu} \propto \nu_{\lambda}^{\alpha}$, with $\alpha_{\lambda} = 1$. This power-law dependence approximately corresponds to a H I column density distribution function proportional to $N^{-4/3}$. This distribution shape is somewhat flatter than the distribution of lower density Ly α forest absorbers, but consistent with some measurements and models at $z = 2-6$ (Faucher-Giguère et al. 2009; Songaila & Cowie 2010). We note that this connection to the column density distribution is only an approximation, as the shape is likely much more complicated in the relevant range of H I column densities (e.g. Haardt & Madau 2012; O’Meara et al. 2013; Prochaska et al. 2014).

For the ionizing background, at $z < 5$ we adopt the measurements of Γ_{HI} from Becker & Bolton (2013), who calibrated a suite of hydrodynamical simulations to the mean transmitted flux of Ly α derived from a stacking analysis of SDSS quasars (Becker et al. 2013), and comprehensively accounted for various sources of systematic uncertainty. At $z > 5$, we use the constraints on Γ_{HI} from Davies et al. (2024), who fit a fluctuating ionizing background model (Davies & Furlanetto 2016) to the Ly α forest opacity distributions from Bosman et al. (2022). To determine the specific intensity at the hydrogen-ionizing edge J_{HI} required by equation (16), we assume that the spectrum of the hydrogen-ionizing

background (i.e. $\nu_{\text{HI}} < \nu < 4\nu_{\text{HI}}$) is described by a power-law shape $J_{\nu} \propto \nu^{-\alpha_b}$ with $\alpha_b = 1.0$. This spectral shape is consistent with an intrinsic ionizing emissivity proportional to ν^{-2} (cf. Becker & Bolton 2013; D’Aloisio et al. 2019) filtered through the absorber distribution giving rise to $\lambda_{\nu} \propto \nu^1$ as assumed above. We then determine the corresponding J_{HI} by requiring that the observed Γ_{HI} is reproduced by

$$\Gamma_{\text{HI}} = 4\pi \int_{\nu_{\text{HI}}}^{4\nu_{\text{HI}}} \frac{J_{\text{HI}}(\nu/\nu_{\text{HI}})^{-\alpha_b}}{h\nu} \sigma_{\text{HI}}(\nu) d\nu, \quad (17)$$

where $\sigma_{\text{HI}}(\nu)$ is the hydrogen photoionization cross-section from Verner et al. (1996).

We note that the mean free path measurements from Zhu et al. (2023) are derived assuming specific values of the hydrogen photoionization rate (and its uncertainty) from Gaikwad et al. (2023). To ensure self-consistency, we recompute the mean free path and corresponding uncertainties using the Davies et al. (2024) constraints on $\Gamma_{\text{HI}}(z)$, but note that this does not make a substantial difference to our results.

3.2. Estimates of the effective clumping factor

With the ionizing background strength and mean free path in hand, we can now proceed to compute the clumping factor following Section 2. Specifically, we evaluate equation (16) using the mean free path measured by Worseck et al. (2014) (i.e. the power-law fit from $z = 2-5$) and Zhu et al. (2023), and the ionizing background intensity implied by the photoionization rate measurements of Becker & Bolton (2013) and Davies et al. (2024), with assumed frequency dependencies $\lambda_{\nu} \propto \nu$ and $J_{\nu} \propto \nu^{-1}$.

We show the resulting estimates of C from $z = 2-6$ in Figure 1. The error bars at $z < 5$ include only the uncertainty in Γ_{HI} from Becker & Bolton (2013), while at $z > 5$ they include both the uncertainty in Γ_{HI} from Davies et al. (2024) and in λ_{mfp} from Zhu et al. (2023). We find a remarkably constant value of $C \sim 10-15$ across the entire redshift range, with an average value of $C \approx 12$ at $z = 5-6$, well above the simulation-calibrated prescriptions often used in the literature ($C \sim 3$). While the short mean free path at $z = 6$ suggests a rather high value $C \sim 17$, its corresponding uncertainty is large enough to be consistent with all lower redshifts.

We note that at $z \lesssim 4$ we expect that our assumption of local photoionization equilibrium becomes increasingly incorrect. The mean free path at this time is long enough that the local source approximation is no longer valid (see, e.g., the discussion in Becker & Bolton 2013), so the photons being absorbed at a given epoch were emitted at a substantially earlier time. In addition,

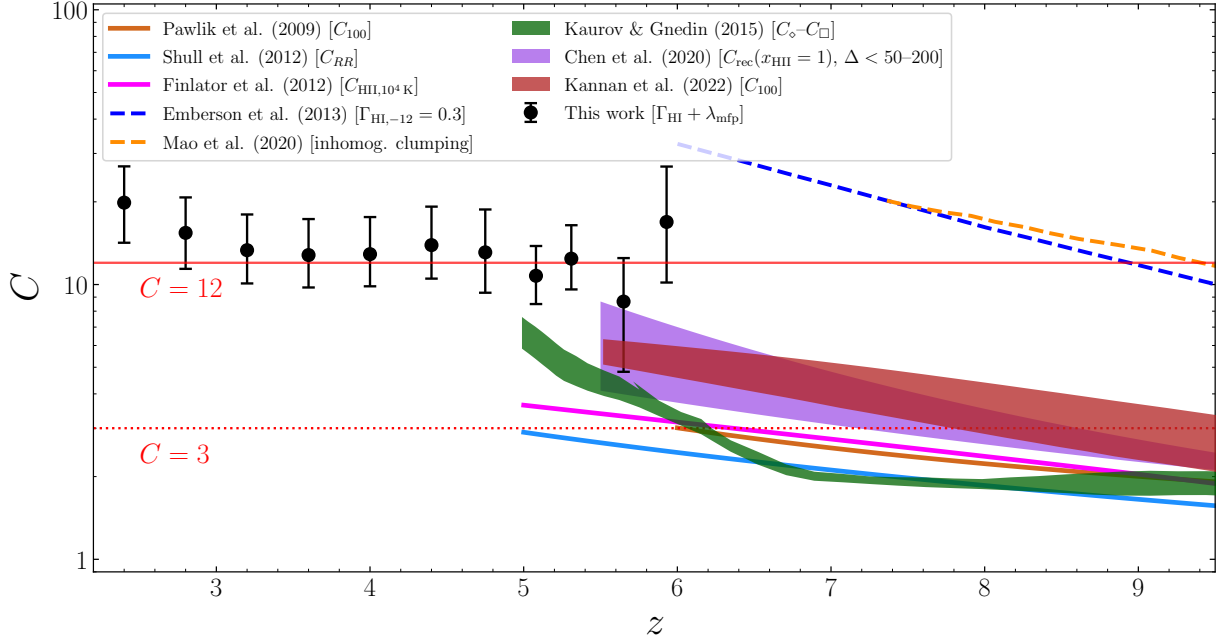


Figure 2. Comparison between the C estimates from this work (black points) and from various cosmological simulations. The solid curves show fits to the simulations from Pawlik et al. (2009) in brown, Shull et al. (2012) in light blue, and Finlator et al. (2012) in pink. The shaded regions show ranges in C estimates from Kaurov & Gnedin (2015) in green and Chen et al. (2020) in purple, where for the latter we have set the ionized fraction to unity to mimic our assumptions. The dashed curves show simulations without photoionization heating, with the small-box adiabatic hydrodynamical simulation from Emberson et al. (2013) in blue and the N-body simulations from Mao et al. (2020) in orange.

as the mean free path increases an increasing fraction of ionizing photons will redshift below ν_{HI} before encountering a hydrogen atom. Neglecting these effects is likely the cause for the upturn in our C estimates at $z < 3$ visible in Figure 1.

3.3. Comparison to simulations

In Figure 2, we compare our estimates of C to various determinations of C -like quantities in the literature. The solid curves from Pawlik et al. (2009), Shull et al. (2012), and Finlator et al. (2012) represent the basis behind the commonly-assumed values of $C = 2$ – 3 , with the ranges of estimates from more recent simulations by Kaurov & Gnedin (2015), Chen et al. (2020), and Kannan et al. (2022) shown as shaded regions with moderately higher values up to $C \sim 5$ at $z = 5$ – 6 . All of these works compute the clumping factor in different ways, but in principle they are all designed to fulfill the same role: to quantify the effect of the sink term on the progression of reionization in equation (1).

The dashed curves in Figure 2 show clumping factors measured from simulations without any contribution from photoionization heating, with Emberson et al. (2013) employing small-volume adiabatic hydrodynamical simulations and Mao et al. (2020, see also Bianco et al. 2021) using a combination of small and large N-

body simulations. These curves can be considered to be theoretical “maximum” values for C , and our estimates lie comfortably below them.

Why, then, do we recover such a large value for C compared to the commonly-accepted value from simulations? In the absence of an unforeseen source of bias in our approach, it is possible that the C measured in simulations is not directly comparable to our value of C due to a difference in definition. Simulations are careful to compute C without including dense gas inside of halos, to avoid double-counting this gas which could be responsible for the galactic escape fraction. This is typically implemented as a density threshold, e.g. C_{100} from Pawlik et al. (2009) is measured from gas with overdensity $\Delta < 100$. Other works include cuts on the temperature and ionization state of the gas (e.g. Finlator et al. 2012; Kaurov & Gnedin 2015).

But this dense gas masking ignores the crucial possibility that dense halo gas can also be illuminated from the *outside* by the UV background, and potentially make up a substantial fraction of the opacity to ionizing photons streaming through the IGM. The mean free path measured in stacked quasar spectra (e.g. Prochaska et al. 2009; Worseck et al. 2014; Becker et al. 2021; Zhu et al. 2023) or from the H I column density distribution (Rudie et al. 2013; Prochaska et al. 2014), includes encounters

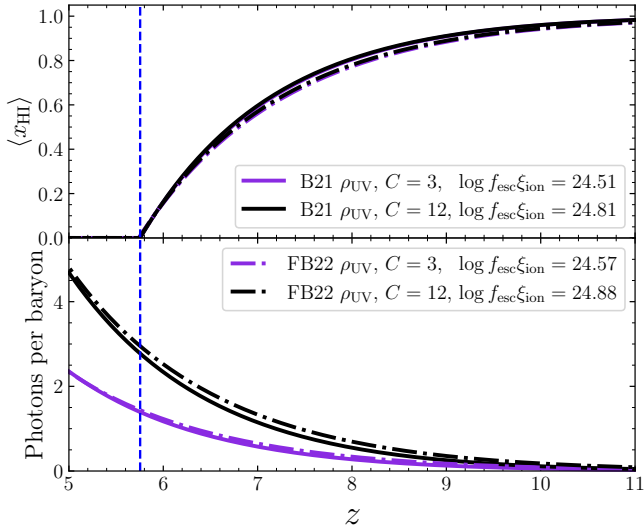


Figure 3. Reionization histories (upper panel) computed using equation (1) with $C = 3$ (purple) and $C = 12$ (black) and the cumulative number of ionizing photons per baryon (lower panel). We integrate the UV LFs from Bouwens et al. (2021, solid) and Finkelstein & Bagley (2022, dot-dashed) down to $M_{\text{UV}} = -13$ to compute the UV luminosity density, and multiply by fixed values of $f_{\text{esc}}\xi_{\text{ion}}$ given in the legend to calibrate \dot{n}_{ion} to reach $Q = 0.9$ at $z = 5.9$, which then finishes reionization at $z \approx 5.7$ (vertical dashed line). While our estimate of $C = 12$ does not affect the reionization history compared to the classical assumption of $C = 3$ in this scenario, it requires a factor ~ 2 higher total photon output from galaxies to finish reionization.

of ionizing photons with all gas without any regard for whether it is associated with a galaxy.

Recent simulations by Cain et al. (2023) which take into account the effect of IGM small-scale ($\sim \text{kpc}$) structure and its relaxation dynamics after reionization heating (Park et al. 2016; D’Aloisio et al. 2020; Chan et al. 2024), have found that applying a clumping factor $C = 5$ to their coarse 1 Mpc-resolution simulation provides a decent match to their more sophisticated sink modeling. On the surface, this value is substantially lower than our estimates, but recall that our C is defined *globally* – this distinction is important, because the locally-defined C can be much smaller than the global one (Raićević & Theuns 2011). In fact, the scale-dependence of the clumping factor found by Kaurov & Gnedin (2015) suggests that the global C is ~ 2 times larger than the local C on ~ 1 Mpc scales, implying that our estimate for the (global) C is reasonably consistent with the model from Cain et al. (2023).

4. IMPLICATIONS FOR REIONIZATION

Fundamentally, the purpose of estimating this particular definition of the clumping factor is to explore

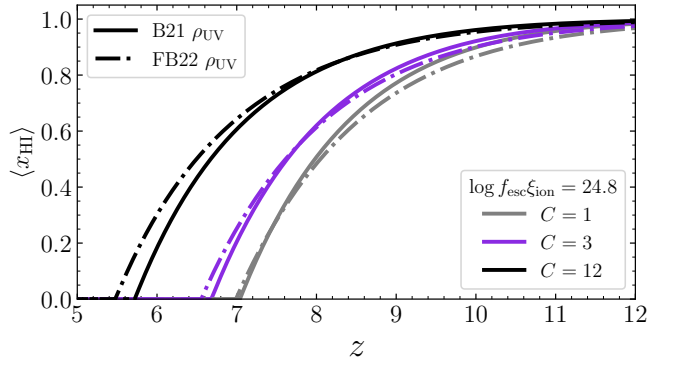


Figure 4. Similar to the upper panel of Figure 3 but keeping $f_{\text{esc}}\xi_{\text{ion}}$ fixed to $10^{24.8}$ erg/Hz, and including the case of a uniform IGM ($C = 1$, grey).

what implications the short mean free path of ionizing photons at $z = 6$ has for the reionization history, and particularly, for the requirements on the number of ionizing photons that must have been emitted to complete the process. The semi-numerical simulations in Paper I examined this in the context of the way a short mean free path inhibits the ionization of the last remaining voids; here, instead, we consider solely the effect of the additional recombinations inside of ionized gas from the large clumping factor implied by IGM observations at $z = 5\text{--}6$ as shown above. While analytically convenient, this choice comes at the expense of neglecting the effect of the spatial offset between ionizing sources and the last patches of neutral gas at the end of reionization (Paper I; Davies & Furlanetto 2022); we leave a closer look at that effect to future work. In this section we will consider the impact of our high value of $C = 12$ on reionization calculations involving equation (1).

We must first consider our model for the sources, i.e. \dot{n}_{ion} (equation 2). We compute $\rho_{\text{UV}}(z)$ from the evolving UV LF parameterizations by Bouwens et al. (2021) and Finkelstein & Bagley (2022), extrapolating up to $z = 15$, and integrating down to a fiducial limiting UV magnitude of $M_{\text{UV}} = -13$. The redshift evolution of the Finkelstein & Bagley (2022) LF includes a strongly evolving suppression at the faint end leading to a rapid decline in the UV luminosity density at the upper end of (and beyond) their fitting range at $z \gtrsim 9$. We thus extrapolate to higher redshift with a double-power-law fit to the evolution at $5 < z < 8.5$, although we note that this makes little difference to our main results.

We can now explore the consequences for the reionization history, integrating equation (1) across cosmic time. We adopt clumping factors of $C = 3$, representing the traditional approach, and $C = 12$, as determined in this work. We then tune the product of the ionizing escape

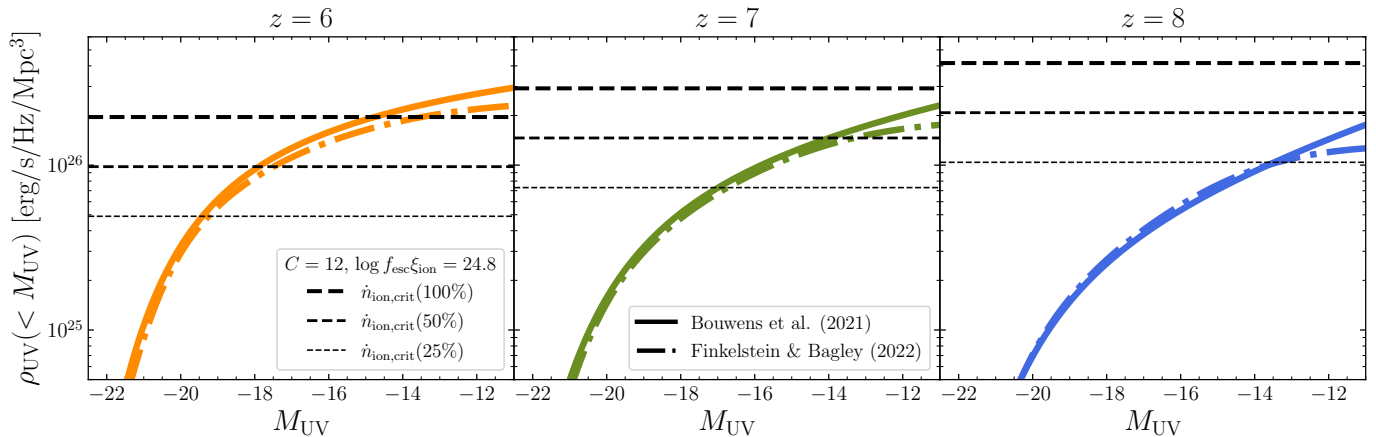


Figure 5. Required UV luminosity density from galaxies in order to maintain the Universe fully, 50%, and 25% ionized (thick to thin dashed lines). Assuming an effective ionization production $f_{\text{esc}}\xi_{\text{ion}} = 10^{24.8}$ erg/Hz and a clumping factor $C = 12$, the integrated light from galaxies down to $M_{\text{UV}} = -13$ is capable of maintaining a fully ionized the Universe at $z = 6$, but only $< 50\%$ at $z = 8$. The results depend only weakly on the choice of UV LF, Bouwens et al. (2021) (solid) or Finkelstein & Bagley (2022) (long-dashed).

fraction and ionizing efficiency $f_{\text{esc}}\xi_{\text{ion}}$ in each case to reach a neutral fraction of 10% at $z = 5.9$, consistent with the Ly α forest dark pixel constraint from McGreer et al. (2015) and with the model from Paper I, leading to a late end to reionization consistent with the most recent constraints from the Ly α forest (Zhu et al. 2021, 2022, 2024; Bosman et al. 2022; Spina et al. 2024).

The resulting reionization histories are shown in the top panel of Figure 3. At this fixed endpoint of reionization, and with our particular models for $\dot{n}_{\text{ion}}(z)$, increasing the clumping factor from $C = 3$ to $C = 12$ has a negligible effect on the reionization history at earlier times. In the lower panel of Figure 3, we show the corresponding integrated number of ionizing photons per baryon. Assuming $C = 3$ requires 1.3–1.5 photons per baryon to complete reionization, while with $C = 12$ the number doubles to 2.5–3.0 photons per baryon. This elevated photon budget is nevertheless still slightly below the nominal range from Paper I, but it is very similar to the dynamic sink radiative transfer models of Cain et al. (2021). This number is also consistent with the total number of recombinations at the end of reionization (i.e. the number of emitted photons per baryon minus one) in the CROC radiation hydrodynamical simulations (Gnedin 2022, 2024).

More generally, if we remove the restriction on the endpoint of reionization, we can explore how different values of C change the reionization history at fixed $\dot{n}_{\text{ion}}(z)$. In Figure 4, we show reionization histories similar to Figure 3 but with a fixed $f_{\text{esc}}\xi_{\text{ion}} = 10^{24.8}$ erg/Hz, corresponding to e.g. a model with $\xi_{\text{ion}} = 10^{25.8}$ erg/Hz, consistent with a recent determination for UV-faint galaxies with JWST (Atek et al. 2024), and $f_{\text{esc}} = 0.1$,

consistent with direct measurements of Lyman continuum photons from Lyman-break galaxies at $z \sim 3$ (Pahl et al. 2021). While the conventional assumption of $C = 3$ only modestly postpones the end of reionization by $\Delta z \sim 0.3$ relative to a uniform IGM ($C = 1$), our fiducial $C = 12$ delays its completion by $\Delta z \gtrsim 1$.

Next, we examine the commonly-used criterion for reionization to remain complete, defined by setting $Q = 1$ and $dQ/dt = 0$ in equation (1):

$$\dot{n}_{\text{ion,crit}} \geq C \langle n_{\text{H}} \rangle^2 \alpha_{\text{HII}}. \quad (18)$$

We note that this expression can be re-stated as a criterion that reionization *progresses* at a given value of the ionized fraction (e.g. Cullen et al. 2024),

$$\dot{n}_{\text{ion,crit}}(Q) \geq QC \langle n_{\text{H}} \rangle^2 \alpha_{\text{HII}} = Q \times \dot{n}_{\text{ion,crit}}. \quad (19)$$

i.e. for the ionized fraction to increase with time, the number of new ionizations must be larger than the number of recombinations within the ionized phase of the IGM.

In Figure 5, we compare the critical values of ionizing photon emissivity for ionized fractions of 25%–100% at $z = 6$ –8 with the corresponding emissivity calculated from the UV LFs versus the UV magnitude integration limit. As in Figure 4, we assume $f_{\text{esc}}\xi_{\text{ion}} = 10^{24.8}$ erg/Hz. Under this assumption, galaxies at $z = 6$ can maintain reionization provided that ionizing photons escape from galaxies as faint as $M_{\text{UV}} \sim -14$, while at $z = 7$ and $z = 8$ this would only be sufficient to continue reionizing the universe at ionized fractions of 50% and 25%, respectively.

5. SUMMARY & CONCLUSION

In this work, we have explored the implications of the short mean free path of ionizing photons at $z \approx 6$ (Becker et al. 2021; Zhu et al. 2023) for the recombination rate in the intergalactic medium as a whole, quantified by the clumping factor C . We first build an analytic connection between the mean free path and the recombination rate with minimal assumptions. The number density of ionizing photons in the optically-thin IGM can be derived from the hydrogen photoionization rate Γ_{HI} measured from the Ly α forest, and the rate at which these photons perform an ionization can be derived from the photon lifetime implied by the typical distance they travel before being absorbed, i.e. the mean free path. A global value for C can then be estimated by comparing this rate to the recombination rate expected for a uniform IGM at the cosmic mean density.

We find a characteristic value of $C \approx 12$ at $z = 5\text{--}6$ that is well in excess of the $C = 3$ assumption commonly made in the literature based on cosmological radiation-hydrodynamics simulations. Surprisingly, this elevated value persists to later times, consistent with non-evolution down to $z \sim 2.5$. We tentatively attribute our higher value of C to the way in which simulation analyses explicitly neglect dense gas within galaxy halos. While such an exclusion appears necessary to avoid double-counting the gas responsible for the galactic escape fraction, it ignores the fact that this dense gas can still absorb *external* photons streaming through the IGM, and thus play an important role in determining the total budget of recombinations.

Compared to the typical assumption of $C = 3$, we find that late-ending reionization histories with $C = 12$

require roughly twice as many ionizing photons to complete the process at $z \lesssim 6$. However, recent observations of the ionizing efficiency of $z > 6$ galaxies from JWST (e.g. Simmonds et al. 2024) and scaling relations for the ionizing escape fraction from low-redshift Lyman continuum leakers (e.g. Chisholm et al. 2022) imply a tremendous *excess* in the ionizing photon budget (Muñoz et al. 2024). Due to the difference in our assumed recombination coefficient, the recombination rate in our fiducial model with $C = 12$ is comparable to that of the $C = 20$ model explored by Muñoz et al. (2024) in which reionization still ends quite early at $z \sim 7.5$.

We note also that the clumping factor may not provide a complete picture of the number of photons required to complete the reionization process. As shown in Paper I, the fact that the ionizing sources and neutral islands are physically offset from one another implies a large degree of attenuation, requiring ~ 6 photons per baryon to reach a neutral fraction of $x_{\text{HI}} \sim 10\%$ at $z \sim 6$; about a factor of two higher than our fiducial model here with $C = 12$. It is possible that both a large recombination rate and a consideration of the physical offset are required to reconcile the copious ionizing photon production of the first galaxies with current constraints on the reionization history.

The manuscript was completed following productive discussions with Girish Kulkarni, Laura Keating, Anson D’Aloisio, and Christopher Cain at the NORDITA workshop programme “Cosmic Dawn at High Latitudes”.

SEIB is supported by the Deutsche Forschungsgemeinschaft (DFG) under Emmy Noether grant number BO 5771/1-1.

APPENDIX

A. SYSTEMATIC VARIATION WITH FREQUENCY DEPENDENCE ASSUMPTIONS

The derivation of the effective global clumping factor in § 2 relies on two assumptions of frequency dependence: the spectral index of the UV background intensity ($J_\nu \propto \nu^{-\alpha_b}$) and the mean free path ($\lambda_\nu \propto \nu^{\alpha_\lambda}$). These two indices are not completely independent – at higher redshifts, the connection can be described via the absorption-limited approximation $J_\nu \propto \epsilon_\nu \lambda_\nu$ (Meiksin & White 2003), where $\epsilon_\nu \propto \nu^{-\alpha_\epsilon}$ is the specific ionizing emissivity of the sources. There is a further frequency dependence in our conversion from the constraints on Γ_{HI} from the Ly α forest to J_{HI} , which involves an integral over the hydrogen photoionization cross-section (equation 17). Approximating the cross-section as $\sigma_{\text{HI}} \propto \nu^{-3}$, the combined frequency dependent term can be written as

$$C(\alpha_b, \alpha_\lambda) \propto \frac{\alpha_b + 3}{1 - 4^{\alpha_b + 3}} \frac{1 - 4^{\alpha_b + \alpha_\lambda}}{\alpha_b + \alpha_\lambda}, \quad (\text{A1})$$

although in practice we integrate over the full form of the photoionization cross-section from Verner et al. (1996).

In Figure 6, we show the full frequency dependence of the clumping factor calculation as a function of α_b for different values of α_λ , taking into account the frequency dependencies in equation (15) and equation (17). Constant values of $\alpha_\epsilon = \alpha_b + \alpha_\lambda$ are indicated, showing the interplay between these three quantities and the estimated clumping factor.

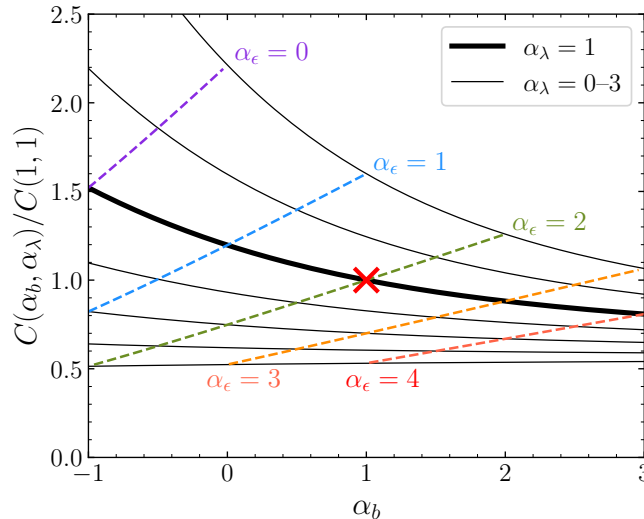


Figure 6. Effect of different frequency dependence assumptions on the estimated clumping factor relative to our fiducial choice of $\alpha_b = 1$ and $\alpha_\lambda = 1$ (red cross). The thick curve shows the variation with α_b at fixed $\alpha_\lambda = 1$, with thin curves showing $\alpha_\lambda = 0-3$ (top to bottom) in steps of 0.5. The dashed colored lines show fixed values of $\alpha_\epsilon = \alpha_b + \alpha_\lambda$, where our fiducial choice corresponds to $\alpha_\epsilon = 2$.

Values of C as low as half of our fiducial estimates are possible only if the mean free path increases sharply with frequency.

We note that the column density distribution assumed in modern cosmological radiative transfer calculations is not a single power-law, but instead described by a piecewise series of power-laws surrounding the most relevant H I column densities within ± 2 dex of the $N_{\text{LLS}} = 10^{17.2} \text{ cm}^{-2}$ (Haardt & Madau 2012; Puchwein et al. 2019; Faucher-Giguère 2020). In these models, the slope of the distribution at N_{LLS} can be very steep; for example, Puchwein et al. (2019) adopt $f(N) \propto N^{-1.95}$ in the range $10^{16}-10^{18} \text{ cm}^{-2}$. Analytically, this should result in an extremely steep dependence of the mean free path with frequency, with $\alpha_\lambda \sim 3$. Instead, we find that the (no longer power-law) frequency dependence arising from integrating over their column density distribution model at $z = 6$ is better approximated by $\alpha_\lambda \sim 1.6$ close to ν_{HI} , turning over to $\alpha_\lambda < 1$ above $2\nu_{\text{HI}}$. Self-consistently adopting this parameterization for λ_ν in our estimation of the clumping factor in equation (15), including the resulting non-power-law shape of J_ν , would reduce our C from 12 to 10. However, a modest hardening of the source spectrum to $\alpha_\epsilon = 1.2$ would return C to 12.

REFERENCES

- Atek, H., Labbé, I., Furtak, L. J., et al. 2024, *Nature*, 626, 975, doi: [10.1038/s41586-024-07043-6](https://doi.org/10.1038/s41586-024-07043-6)
- Becker, G. D., & Bolton, J. S. 2013, *MNRAS*, 436, 1023, doi: [10.1093/mnras/stt1610](https://doi.org/10.1093/mnras/stt1610)
- Becker, G. D., D’Aloisio, A., Christenson, H. M., et al. 2021, *MNRAS*, 508, 1853, doi: [10.1093/mnras/stab2696](https://doi.org/10.1093/mnras/stab2696)
- Becker, G. D., Hewett, P. C., Worseck, G., & Prochaska, J. X. 2013, *MNRAS*, 430, 2067, doi: [10.1093/mnras/stt031](https://doi.org/10.1093/mnras/stt031)
- Bianco, M., Iliev, I. T., Ahn, K., et al. 2021, *MNRAS*, 504, 2443, doi: [10.1093/mnras/stab787](https://doi.org/10.1093/mnras/stab787)
- Bosman, S. E. I. 2021, arXiv e-prints, arXiv:2108.12446. <https://arxiv.org/abs/2108.12446>
- Bosman, S. E. I., Davies, F. B., Becker, G. D., et al. 2022, *MNRAS*, 514, 55, doi: [10.1093/mnras/stac1046](https://doi.org/10.1093/mnras/stac1046)
- Bouwens, R. J., Oesch, P. A., Stefanon, M., et al. 2021, *AJ*, 162, 47, doi: [10.3847/1538-3881/abf83e](https://doi.org/10.3847/1538-3881/abf83e)
- Cain, C., D’Aloisio, A., Gangolli, N., & Becker, G. D. 2021, *ApJL*, 917, L37, doi: [10.3847/2041-8213/ac1ace](https://doi.org/10.3847/2041-8213/ac1ace)
- Cain, C., D’Aloisio, A., Gangolli, N., & McQuinn, M. 2023, *MNRAS*, 522, 2047, doi: [10.1093/mnras/stad1057](https://doi.org/10.1093/mnras/stad1057)
- Chan, T. K., Benítez-Llambay, A., Theuns, T., Frenk, C., & Bower, R. 2024, *MNRAS*, 528, 1296, doi: [10.1093/mnras/stae114](https://doi.org/10.1093/mnras/stae114)
- Chen, N., Doussot, A., Trac, H., & Cen, R. 2020, *ApJ*, 905, 132, doi: [10.3847/1538-4357/abc890](https://doi.org/10.3847/1538-4357/abc890)
- Chisholm, J., Saldana-Lopez, A., Flury, S., et al. 2022, *MNRAS*, 517, 5104, doi: [10.1093/mnras/stac2874](https://doi.org/10.1093/mnras/stac2874)
- Cullen, F., McLeod, D. J., McLure, R. J., et al. 2024, *MNRAS*, 531, 997, doi: [10.1093/mnras/stae1211](https://doi.org/10.1093/mnras/stae1211)

- D'Aloisio, A., McQuinn, M., Maupin, O., et al. 2019, *ApJ*, 874, 154, doi: [10.3847/1538-4357/ab0d83](https://doi.org/10.3847/1538-4357/ab0d83)
- D'Aloisio, A., McQuinn, M., Trac, H., Cain, C., & Mesinger, A. 2020, *ApJ*, 898, 149, doi: [10.3847/1538-4357/ab9f2f](https://doi.org/10.3847/1538-4357/ab9f2f)
- Davies, F. B., Bosman, S. E. I., Furlanetto, S. R., Becker, G. D., & D'Aloisio, A. 2021, *ApJL*, 918, L35, doi: [10.3847/2041-8213/ac1ffb](https://doi.org/10.3847/2041-8213/ac1ffb)
- Davies, F. B., & Furlanetto, S. R. 2016, *MNRAS*, 460, 1328, doi: [10.1093/mnras/stw931](https://doi.org/10.1093/mnras/stw931)
- . 2022, *MNRAS*, 514, 1302, doi: [10.1093/mnras/stac1005](https://doi.org/10.1093/mnras/stac1005)
- Davies, F. B., Bosman, S. E. I., Gaikwad, P., et al. 2024, *ApJ*, 965, 134, doi: [10.3847/1538-4357/ad1d5d](https://doi.org/10.3847/1538-4357/ad1d5d)
- Emberson, J. D., Thomas, R. M., & Alvarez, M. A. 2013, *ApJ*, 763, 146, doi: [10.1088/0004-637X/763/2/146](https://doi.org/10.1088/0004-637X/763/2/146)
- Erkal, D. 2015, *MNRAS*, 451, 904, doi: [10.1093/mnras/stv980](https://doi.org/10.1093/mnras/stv980)
- Faucher-Giguère, C.-A. 2020, *MNRAS*, 493, 1614, doi: [10.1093/mnras/staa302](https://doi.org/10.1093/mnras/staa302)
- Faucher-Giguère, C.-A., Lidz, A., Zaldarriaga, M., & Hernquist, L. 2009, *ApJ*, 703, 1416, doi: [10.1088/0004-637X/703/2/1416](https://doi.org/10.1088/0004-637X/703/2/1416)
- Finkelstein, S. L., & Bagley, M. B. 2022, *ApJ*, 938, 25, doi: [10.3847/1538-4357/ac89eb](https://doi.org/10.3847/1538-4357/ac89eb)
- Finlator, K., Oh, S. P., Özel, F., & Davé, R. 2012, *MNRAS*, 427, 2464, doi: [10.1111/j.1365-2966.2012.22114.x](https://doi.org/10.1111/j.1365-2966.2012.22114.x)
- Furlanetto, S. R., Zaldarriaga, M., & Hernquist, L. 2004, *ApJ*, 613, 1, doi: [10.1086/423025](https://doi.org/10.1086/423025)
- Gaikwad, P., Haehnelt, M. G., Davies, F. B., et al. 2023, *MNRAS*, 525, 4093, doi: [10.1093/mnras/stad2566](https://doi.org/10.1093/mnras/stad2566)
- Gnedin, N. Y. 2022, *ApJ*, 937, 17, doi: [10.3847/1538-4357/ac8d0a](https://doi.org/10.3847/1538-4357/ac8d0a)
- . 2024, *ApJ*, 963, 150, doi: [10.3847/1538-4357/ad298e](https://doi.org/10.3847/1538-4357/ad298e)
- Gnedin, N. Y., & Ostriker, J. P. 1997, *ApJ*, 486, 581, doi: [10.1086/304548](https://doi.org/10.1086/304548)
- Gunn, J. E., & Peterson, B. A. 1965, *ApJ*, 142, 1633, doi: [10.1086/148444](https://doi.org/10.1086/148444)
- Haardt, F., & Madau, P. 2012, *ApJ*, 746, 125, doi: [10.1088/0004-637X/746/2/125](https://doi.org/10.1088/0004-637X/746/2/125)
- Iliev, I. T., Mellema, G., Shapiro, P. R., & Pen, U.-L. 2007, *MNRAS*, 376, 534, doi: [10.1111/j.1365-2966.2007.11482.x](https://doi.org/10.1111/j.1365-2966.2007.11482.x)
- Iliev, I. T., Scannapieco, E., & Shapiro, P. R. 2005, *ApJ*, 624, 491, doi: [10.1086/429083](https://doi.org/10.1086/429083)
- Izotov, Y. I., Schaerer, D., Thuan, T. X., et al. 2016, *MNRAS*, 461, 3683, doi: [10.1093/mnras/stw1205](https://doi.org/10.1093/mnras/stw1205)
- Ji, Z., Giavalisco, M., Vanzella, E., et al. 2020, *ApJ*, 888, 109, doi: [10.3847/1538-4357/ab5fdc](https://doi.org/10.3847/1538-4357/ab5fdc)
- Kannan, R., Garaldi, E., Smith, A., et al. 2022, *MNRAS*, 511, 4005, doi: [10.1093/mnras/stab3710](https://doi.org/10.1093/mnras/stab3710)
- Kaurov, A. A., & Gnedin, N. Y. 2015, *ApJ*, 810, 154, doi: [10.1088/0004-637X/810/2/154](https://doi.org/10.1088/0004-637X/810/2/154)
- Madau, P. 2017, *ApJ*, 851, 50, doi: [10.3847/1538-4357/aa9715](https://doi.org/10.3847/1538-4357/aa9715)
- Madau, P., Haardt, F., & Rees, M. J. 1999, *ApJ*, 514, 648, doi: [10.1086/306975](https://doi.org/10.1086/306975)
- Mao, Y., Koda, J., Shapiro, P. R., et al. 2020, *MNRAS*, 491, 1600, doi: [10.1093/mnras/stz2986](https://doi.org/10.1093/mnras/stz2986)
- McGreer, I. D., Mesinger, A., & D'Odorico, V. 2015, *MNRAS*, 447, 499, doi: [10.1093/mnras/stu2449](https://doi.org/10.1093/mnras/stu2449)
- McQuinn, M., Oh, S. P., & Faucher-Giguère, C.-A. 2011, *ApJ*, 743, 82, doi: [10.1088/0004-637X/743/1/82](https://doi.org/10.1088/0004-637X/743/1/82)
- Meiksin, A., & White, M. 2003, *MNRAS*, 342, 1205, doi: [10.1046/j.1365-8711.2003.06624.x](https://doi.org/10.1046/j.1365-8711.2003.06624.x)
- Muñoz, J. B., Mirocha, J., Chisholm, J., Furlanetto, S. R., & Mason, C. 2024, arXiv e-prints, arXiv:2404.07250, doi: [10.48550/arXiv.2404.07250](https://doi.org/10.48550/arXiv.2404.07250)
- Ning, Y., Cai, Z., Jiang, L., et al. 2023, *ApJL*, 944, L1, doi: [10.3847/2041-8213/acb26b](https://doi.org/10.3847/2041-8213/acb26b)
- O'Meara, J. M., Prochaska, J. X., Worseck, G., Chen, H.-W., & Madau, P. 2013, *ApJ*, 765, 137, doi: [10.1088/0004-637X/765/2/137](https://doi.org/10.1088/0004-637X/765/2/137)
- Pahl, A. J., Shapley, A., Steidel, C. C., Chen, Y., & Reddy, N. A. 2021, *MNRAS*, 505, 2447, doi: [10.1093/mnras/stab1374](https://doi.org/10.1093/mnras/stab1374)
- Park, H., Shapiro, P. R., Choi, J.-h., et al. 2016, *ApJ*, 831, 86, doi: [10.3847/0004-637X/831/1/86](https://doi.org/10.3847/0004-637X/831/1/86)
- Pawlik, A. H., Schaye, J., & van Scherpenzeel, E. 2009, *MNRAS*, 394, 1812, doi: [10.1111/j.1365-2966.2009.14486.x](https://doi.org/10.1111/j.1365-2966.2009.14486.x)
- Planck Collaboration, Aghanim, N., Akrami, Y., et al. 2020, *A&A*, 641, A6, doi: [10.1051/0004-6361/201833910](https://doi.org/10.1051/0004-6361/201833910)
- Prieto-Lyon, G., Strait, V., Mason, C. A., et al. 2023, *A&A*, 672, A186, doi: [10.1051/0004-6361/202245532](https://doi.org/10.1051/0004-6361/202245532)
- Prochaska, J. X., Madau, P., O'Meara, J. M., & Fumagalli, M. 2014, *MNRAS*, 438, 476, doi: [10.1093/mnras/stt2218](https://doi.org/10.1093/mnras/stt2218)
- Prochaska, J. X., Worseck, G., & O'Meara, J. M. 2009, *ApJL*, 705, L113, doi: [10.1088/0004-637X/705/2/L113](https://doi.org/10.1088/0004-637X/705/2/L113)
- Puchwein, E., Haardt, F., Haehnelt, M. G., & Madau, P. 2019, *MNRAS*, 485, 47, doi: [10.1093/mnras/stz222](https://doi.org/10.1093/mnras/stz222)
- Raičević, M., & Theuns, T. 2011, *MNRAS*, 412, L16, doi: [10.1111/j.1745-3933.2010.00993.x](https://doi.org/10.1111/j.1745-3933.2010.00993.x)
- Rudie, G. C., Steidel, C. C., Shapley, A. E., & Pettini, M. 2013, *ApJ*, 769, 146, doi: [10.1088/0004-637X/769/2/146](https://doi.org/10.1088/0004-637X/769/2/146)
- Satyavolu, S., Kulkarni, G., Keating, L. C., & Haehnelt, M. G. 2023, *MNRAS*, 521, 3108, doi: [10.1093/mnras/stad729](https://doi.org/10.1093/mnras/stad729)
- Shull, J. M., Harness, A., Trenti, M., & Smith, B. D. 2012, *ApJ*, 747, 100, doi: [10.1088/0004-637X/747/2/100](https://doi.org/10.1088/0004-637X/747/2/100)

- Simmonds, C., Tacchella, S., Maseda, M., et al. 2023, MNRAS, 523, 5468, doi: [10.1093/mnras/stad1749](https://doi.org/10.1093/mnras/stad1749)
- Simmonds, C., Tacchella, S., Hainline, K., et al. 2024, MNRAS, 527, 6139, doi: [10.1093/mnras/stad3605](https://doi.org/10.1093/mnras/stad3605)
- So, G. C., Norman, M. L., Reynolds, D. R., & Wise, J. H. 2014, ApJ, 789, 149, doi: [10.1088/0004-637X/789/2/149](https://doi.org/10.1088/0004-637X/789/2/149)
- Songaila, A., & Cowie, L. L. 2010, ApJ, 721, 1448, doi: [10.1088/0004-637X/721/2/1448](https://doi.org/10.1088/0004-637X/721/2/1448)
- Spina, B., Bosman, S. E. I., Davies, F. B., Gaikwad, P., & Zhu, Y. 2024, arXiv e-prints, arXiv:2405.12273, doi: [10.48550/arXiv.2405.12273](https://doi.org/10.48550/arXiv.2405.12273)
- Vanzella, E., Nonino, M., Cupani, G., et al. 2018, MNRAS, 476, L15, doi: [10.1093/mnrasl/sly023](https://doi.org/10.1093/mnrasl/sly023)
- Verner, D. A., Ferland, G. J., Korista, K. T., & Yakovlev, D. G. 1996, ApJ, 465, 487
- Worseck, G., Davies, F. B., Hennawi, J. F., & Prochaska, J. X. 2019, ApJ, 875, 111, doi: [10.3847/1538-4357/ab0fa1](https://doi.org/10.3847/1538-4357/ab0fa1)
- Worseck, G., Prochaska, J. X., O'Meara, J. M., et al. 2014, MNRAS, 445, 1745, doi: [10.1093/mnras/stu1827](https://doi.org/10.1093/mnras/stu1827)
- Wu, X., McQuinn, M., Eisenstein, D., & Iršič, V. 2021, MNRAS, 508, 2784, doi: [10.1093/mnras/stab2815](https://doi.org/10.1093/mnras/stab2815)
- Zhu, Y., Becker, G. D., Bosman, S. E. I., et al. 2021, ApJ, 923, 223, doi: [10.3847/1538-4357/ac26c2](https://doi.org/10.3847/1538-4357/ac26c2)
- . 2022, ApJ, 932, 76, doi: [10.3847/1538-4357/ac6e60](https://doi.org/10.3847/1538-4357/ac6e60)
- Zhu, Y., Becker, G. D., Christenson, H. M., et al. 2023, ApJ, 955, 115, doi: [10.3847/1538-4357/aceef4](https://doi.org/10.3847/1538-4357/aceef4)
- Zhu, Y., Becker, G. D., Bosman, S. E. I., et al. 2024, MNRAS, doi: [10.1093/mnrasl/slae061](https://doi.org/10.1093/mnrasl/slae061)